MNRAS **000**, 1–8 (2018) Preprint 5 June 2018 Compiled using MNRAS LATEX style file v3.0

The GALAH Survey and *Gaia* DR2: (Non)existence of four sparse high-latitude open clusters

Janez Kos,[1]★ Gayandhi de Silva,[1,2] Joss Bland-Hawthorn,[1,3,4] Timothy R. Bedding,[1,5] and The GALAH Collaboration,
[1]*Sydney Institute for Astronomy, School of Physics A28, The University of Sydney, NSW 2006, Australia*
[2]*Australian Astronomical Observatory, 105 Delhi Rd, North Ryde, NSW 2113, Australia*
[3]*ARC Centre of Excellence for All Sky Astrophysics in 3 Dimensions (ASTRO-3D), Australia*
[4]*Sydney Astrophotonic Instrumentation Labs, School of Physics, A28, The University of Sydney, NSW 2006, Australia*
[5] *Stellar Astrophysics Centre, Department of Physics and Astronomy, Aarhus University, Denmark*

Accepted XXX. Received YYY; in original form ZZZ

ABSTRACT

Sparse open clusters can be found at high galactic latitudes where loosely populated clusters are more easily detected against the lower stellar background. As bursty star formation takes place in the thin disk, the population of clusters far from the Galactic plane is hard to explain. We combined spectral parameters from the GALAH survey with the *Gaia* DR2 catalogue to study dynamics and chemistry of 5 old sparse high-latitude clusters in more detail. We find that four of them (NGC 1252, NGC 6994, NGC 7772, NGC 7826) - originally classified in 1888 - are not clusters but fluke projections on the sky. Member stars quoted in the literature for these four clusters are unrelated in our multi-dimensional physical parameter space; the published cluster properties are therefore irrelevant. We confirm the existence of morphologically similar NGC 1901 for which we provide a probabilistic membership analysis. An overdensity in three spatial dimensions proves to be enough to reliably detect sparse clusters, but the whole 6-dimensional space must be used to identify members with high confidence, as demonstrated in the case of NGC 1901.

Key words: catalogues – surveys – parallaxes – proper motions – techniques: radial velocities – open clusters and associations

1 INTRODUCTION

The GALAH survey (De Silva et al. 2015; Buder et al. 2018) is a high-resolution (R=28,000), high signal-to-noise ratio (SNR≈100) spectroscopic survey of one million stars. The aim of the survey is to measure abundances of up to 30 elements with a goal to disentangle the chemical history of the Milky Way (Freeman & Bland-Hawthorn 2002). Open clusters are observed in a dedicated program (De Silva et al., 2018, in preparation) associated with the full GALAH survey. Open clusters play a fundamental role in understanding the chemical evolution of stars, since they are almost the only stellar population with homogeneous elemental abundances (De Silva et al. 2006, 2007; Sestito et al. 2007; Bovy 2016) arising from a common birth-time and place. Hence, processes in the evolution of stellar systems are best studied in clusters, including, but not limited, to the initial mass function of stars (Chabrier 2003; Krumholz 2014), the interaction with the disk (Gieles et al. 2007; Gieles & Bastian 2008) or Galactic tidal fields (Baumgardt & Makino 2003), the creation of blue stragglers (Stryker 1993), radial migration (Fujii & Baba 2012), and atomic diffusion (Bertelli Motta et al. 2018). Open clusters have long been considered as representatives of star formation in the Galaxy, since they are mostly found in the thin disk. Open clusters in other components of the Galaxy are rare, and so confirming their reality and measuring their properties is vital for using them to study the aforementioned processes in parts of the Galaxy outside the Galactic plane.

The clusters addressed in this work were believed to be old and far from the Galactic plane. At first glance, this is surprising because the survival time of such clusters is lower than their thin disk

★ E-mail: janez.kos@sydney.edu.au

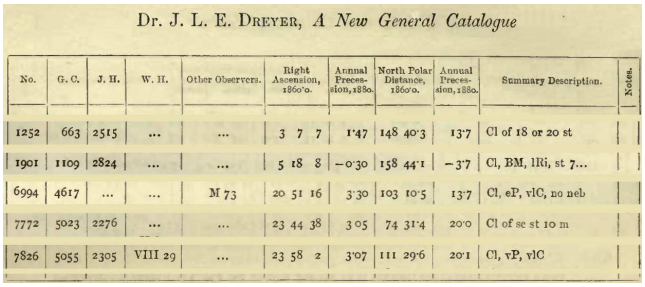

Dr. J. L. E. Dreyer, *A New General Catalogue*

No.	G. C.	J. H.	W. H.	Other Observers.	Right Ascension, 1860·0.	Annual Precession, 1880.	North Polar Distance, 1860·0.	Annual Precession, 1880.	Summary Description.	Notes.
1252	663	2515	...	...	3 7 7	1·47	148 40·3	13·7	Cl of 18 or 20 st	
1901	1109	2824	...	...	5 18 8	−0·30	158 44·1	−3·7	Cl, BM, 1Ri, st 7...	
6994	4617	...	...	M 73	20 51 16	3·30	103 10·5	13·7	Cl, eP, vlC, no neb	
7772	5023	2276	...	...	23 44 38	3·05	74 31·4	20·0	Cl of sc st 10 m	
7826	5055	2305	VIII 29	...	23 58 2	3·07	111 29·6	20·1	Cl, vP, vlC	

Figure 1. For early observers these were without much doubt clusters of stars. The mistake could be attributed to "[...] accidental errors occasionally met with in the observations of the two Herschels, and which naturally arose from the construction of their instruments and the haste with which the observations often necessarily were made." (Dreyer 1888)

counterparts (Martinez-Medina et al. 2017). A simple model where most of the star formation happens in the thin disk has to be updated to explain open clusters at high galactic latitudes, assuming these are real[1]. The prevailing theories are heating of the disk (Gustafsson et al. 2016), soft lifting through resonances (Martinez-Medina et al. 2016), mergers (Kereš et al. 2005; Sancisi et al. 2008), and in-situ formation from high-latitude molecular clouds (Camargo et al. 2016). Sparse clusters are very suitable for testing the above theories because they are numerous and low in mass, and are therefore more likely to be involved in the above processes.

Sparse clusters are the last stage at which we can currently connect the related stars together before they dissipate into the Galaxy. Chemical tagging – the main objective of the GALAH survey – often uses such structures as a final test before attempting to tag field stars. Because sparse clusters are probably dissolving rapidly, we can expect to find many former members far from the cluster centre (Kos et al. 2018; de Silva et al. 2011). If these former members can be found, the dynamics of cluster dissipation and interaction with the Galactic potential could be studied in great detail.

Historically, sparse open clusters and open cluster remnants have been identified based on the aggregation of stars on the sky and their positions in the HR diagram. Spectroscopy was rarely used, possibly because it was too expensive use of telescope time. Massive spectroscopic surveys either did not exist or only included one or a few potential members. Often, there was only one spectroscopically observed star in the cluster, so even for misidentified clusters the values for radial velocity (v_r) and metallicity[2] ([M/H], [Fe/H]) can be found in the literature, even though the most basic spectroscopic inspection of a handful of stars would disprove the existence of the cluster. When identifying the clusters based on the position of stars in the HR diagram, most stars that fell close to the desired isochrone were used. Sparse clusters are often reported at high galactic latitudes, where the density of field stars is low and only a few are needed for an aggregation to stand out. Lacking other information, the phenomenon of pareidolia led early observers to conclude that many "associations" were real (Figure 1). The cluster labels have stuck, however, and several studies have been made of properties of these clusters (see Section 2.2 and references therein).

The amount of available data has increased enormously with *Gaia* DR2. The search for new clusters will now be more reliable, given that precise proper motions and parallax add three more dimensions in which the membership can be established (Koposov et al. 2017; Castro-Ginard et al. 2018; Torrealba et al. 2018; Cantat-Gaudin et al. 2018; Dias et al. 2018).

In Section 2 we review the studied data and explain the methods used to disprove the existence of four clusters and confirm a fifth. Section 3 provides more details about the analysis of the real cluster NGC 1901. In Section 4 we discuss some implications of our findings.

2 EXISTENCE OF CLUSTERS

2.1 Data

Stars observed as a part of the GALAH survey are selected from the 2MASS catalogue (Skrutskie et al. 2006). Depending on the observing mode, all the stars in a 2° field are in a magnitude range $12 < V < 14$ for regular fields and $9 < V < 12$ for bright fields. For some clusters targeted in the dedicated cluster program, we used a custom magnitude range to maximise the number of observed members. The V magnitude is calculated from the 2MASS photometry. In general, the GALAH V magnitude is ~ 0.3 fainter than *Gaia* G magnitude.

Most of the data used in this work comes from the *Gaia* DR2 (Gaia Collaboration et al. 2018), which includes positions, G magnitudes, proper motions and parallaxes for more than 1.3 billion stars. This part of the catalogue is essentially complete for $12 < G < 17$, which is the range where we expect most of the cluster stars discussed in this paper. There are, however, a few members of the four alleged clusters that are brighter than $G = 12$ and are not included in *Gaia* DR2, but do not impact the results of this paper. Radial velocities in *Gaia* DR2 are only given for 7.2 million stars down to $G = 13$. Since the precision of radial velocities is significantly higher in the GALAH survey, we use GALAH values wherever available. Since GALAH has a more limited magnitude range than *Gaia*, there are many stars for which *Gaia* DR2 radial velocities must be used. There are no systematic differences between the two surveys, so we can use whichever velocity is available.

2.2 Clusters

In the fields observed by the GALAH survey, we identified 39 clusters with literature references. Four of them (NGC 1252, NGC 6994, NGC 7772, and NGC 7826) appeared to have no observed members, even though we targeted them based on the data in the literature. All four clusters are sparse, with possibly only ~ 10 members, extended, and at high galactic latitudes. Among the other 35 observed clusters we only found one (NGC 1901) that is morphologically similar to those four and it is most certainly a real open cluster, as confirmed by the literature (Eggen 1996; Pavani et al. 2001; Dias et al. 2002; Carraro et al. 2007; Kharchenko et al. 2013; Conrad et al. 2014) and our own observations. See Table 1 for a list of basic parameters of these five clusters. We observed more clusters at high latitudes (Blanco 1, NGC 2632, M 67, and NGC 1817), but they are all more populated than the five clusters studied here.

NGC 1252 was thought to be metal poor, old (3 Gyr) and far from the Galactic plane ($z = -900$ pc). This would be a unique

[1] Clusters can have high galactic latitude and still be well inside the thin disk if they are close to us. By high-latitude clusters, we mean those that are far from the Galactic plane.

[2] In the literature the metallicity [M/H] and iron abundance [Fe/H] are used interchangeably. We discuss the importance of differentiating them in Section 3.

Table 1. Coordinates of the clusters used in this work. For the non-existing clusters the heliocentric distances d and distances from the Galactic plane z are taken from the literature (see Section 2.2).

Cluster name	α °	δ °	l °	b °	d pc	z pc
NGC 1252	47.704	-57.767	274.084	-50.831	1000	-775
NGC 1901	79.490	-68.342	278.914	-33.644	426.0	-236.0
NGC 6994	314.750	-12.633	35.725	-33.954	620	-345
NGC 7772	357.942	16.247	102.739	-44.273	1500	-1050
NGC 7826	1.321	-20.692	61.875	-77.653	600	-590

object, as no such old clusters are found that far from the Plane (de la Fuente Marcos et al. 2013). It has been argued in the past that this cluster is not real (Baumgardt & Makino 2003).

NGC 6994 was thought to be old (2 to 3 Gyr), fairly far away from the plane ($z = -350$ pc) and dynamically well evolved cluster remnant (Bassino et al. 2000). Carraro (2000); Odenkirchen & Soubiran (2002) successfully argue that NGC 6994 is neither a cluster or a remnant, but only an incidental overdensity of a handful of stars.

NGC 7772 was thought to be 1.5 Gyr old, more than 1 kpc below the Plane and depleted of low mass stars (Carraro 2002).

NGC 7826 has never been studied in detail. It is included in some open cluster catalogues (Dias et al. 2014), where age of 2 Gyr and a distance from the Plane $z = -600$ pc is assumed.

2.3 Literature members

In Tables A1 to A4 we review the available memberships from the literature for clusters NGC 1252, NGC 6994, NGC 7772, and NGC 7826. It is clear they are not clusters and the possible members are in no way related, based on the *Gaia* DR2 parameters and occasionally GALAH radial velocities. We cross matched the lists of members given in the literature to *Gaia* DR2 targets based on positions and magnitude, so all the parameters given in Tables A1 to A4 are from *Gaia* DR2 or GALAH. A small fraction of members in the literature can not be cross-matched with *Gaia* DR2, either because the star is absent from *Gaia* DR2, the coordinates in the literature are invalid, or the members are not clearly marked in a figure or table.

For NGC 1901, we confirm it as a real cluster and provide our own membership analysis in Section 3.

2.4 6D parameter space

Figures 2 and 3 show the six dimensional space (α, δ, μ_α, μ_δ, ϖ, v_r) for all five clusters. We choose to display observed parameters for various reasons; they have lower uncertainties than any derived parameters (actions, orbital parameters, (U,V,W) velocities, etc.), and when the radial velocity is not available we can still use the remaining 5 parameters. There is no common definition of a cluster (or a cluster remnant), but it makes sense that a necessary condition is that the cluster members form an overdensity in space, regardless of the dynamics of the cluster. This is another reason why measurables should be used, as they are already separated into three spatial dimensions and three velocities. We plot positions of stars on the sky (α, δ) in one panel, where an overdensity is hardest to observe, while proper motions are plotted in the second panel and the final two measurables (ϖ and v_r) are plotted in the third panel.

For NGC 1901, we clearly see clumping in both the proper-motion plane and the parallax-radial-velocity plane. An overdensity in all three spatial dimensions is illustrated in Figure 4. One would expect a similar clumping for the other four clusters, if they were real. Instead, we cannot find a single pair of stars (either among the literature members or all *Gaia* stars), that are close together in all six dimensions, even though the overdensity in (α, δ) appears similar to that of NGC 1901.

3 NGC 1901 ANALYSIS

Since NGC 1901 is a real cluster, we provide here our own membership analysis. Firstly, we performed a crude cut in the 6D space ($r < 0.5°$, $0.7 < \mu_\alpha < 2.5\,\mathrm{mas\,yr^{-1}}$, $11.7 < \mu_\delta < 13.5\,\mathrm{mas\,yr^{-1}}$, $1.8 < \varpi < 2.8\,\mathrm{mas}$, and $-2.0 < v_r < 7.0\,\mathrm{km\,s^{-1}}$) to isolate the most probable members. This yielded 80 stars, of which 20 have radial velocities. We used these stars to estimate the mean and spread in every dimension independently (there seems to be no correlation between different dimensions/parameters), which we used to perform a probability analysis. The probability for a star with given parameters (α, δ, μ_α, μ_δ, ϖ, and v_r) to be a member is described by a multivariate Gaussian centred on the values in Table 2. For stars with existing radial velocity measurement we produce two probabilities, one with radial velocity taken into the account (P_{6D}) and one without it (P_{5D}). From the difference between these, we estimate that $\sim 15\%$ of highly probable members based only on the 5D analysis would have their probability reduced significantly if the radial velocity measurement were available. Membership probabilities are given in Table B1.

From the most probable members we can calculate mean parameters and their uncertainties of NGC 1901. In Table 2 we provide the following parameters. Positions α, δ and l, b give cluster centre in celestial and galactic coordinates, respectively. Radii r_0, r_1, and r_2 are estimated visually as described in Kharchenko et al. (2012). King's (King 1962) cluster radius (r_c) and tidal radius (r_t) are fitted, although we were unable to measure the tidal radius with any meaningful confidence. Proper motions, μ_α and μ_δ, are the mean values for the cluster and the uncertainties relate to the mean, not to the dispersion. The radial velocity (v_r) and the velocity dispersion (σ_{v_r}) are measured from a combination of *Gaia* DR2 and GALAH radial velocities. The distance (dist.) is calculated from the parallaxes (ϖ), taking the parallax uncertainties of individual stars into the account. It's uncertainty might be underestimated, if the parallaxes of individual stars have correlated errors. Iron and α abundances ([Fe/H], [α/Fe]) are taken from GALAH and are based on 12 members only. Age (log t) is calculated by isochrone fitting, assuming *Gaia* reddening and extinction (see below).

Putting the most probable members onto the colour-magnitude diagram (Figure 5) and fitting Padova isochrones (Marigo et al. 2017) we can measure the age of the cluster. The precision of the age is somewhat limited, as there are only a few stars close to the turn-off point. The reddening and colour excess as measured by *Gaia* are higher than the literature values and the correlations between the age and reddening/extinction can increase the age uncertainty even further. From fitting the isochrones, we can also tell that there is a significant difference between the metallicity ([M/H] = −0.13) of the best-matching isochrone and the iron abundance ([Fe/H] = −0.32) we measured in the GALAH survey. Forcing the numbers to be the same by compensating for the metallicity by changing colour excess and extinction gives a significantly worse fit of the isochrones. The mismatch between GALAH and *Gaia* DR2 could be due to the

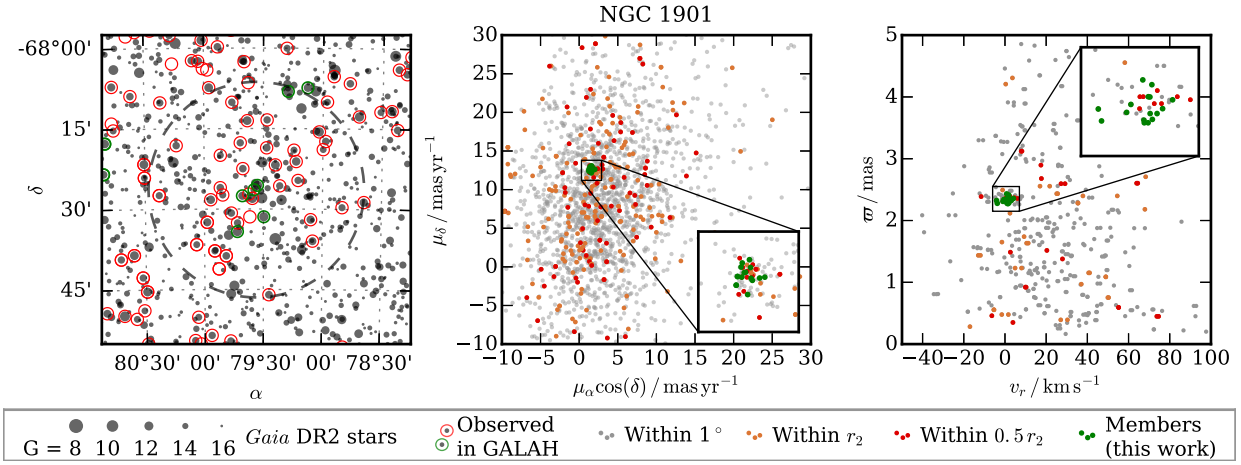

Figure 2. Six dimensional space for stars in and around NGC 1901. Left: Position of *Gaia* DR2 stars with magnitude G<16 (gray) with marked members (circled in green) and stars observed in the GALAH survey (circled in red). The dashed circle marks the cluster radius. Middle: *Gaia* DR2 proper motions for all stars inside a 1° radius from the cluster centre (gray), stars inside r_2 (orange), stars inside 0.5 r_2 (red), and identified members (green). Right: Radial velocity and proper motions for stars that have radial velocity measured either in *Gaia* DR2 or in the GALAH survey. Same colors are used as in the middle panel.

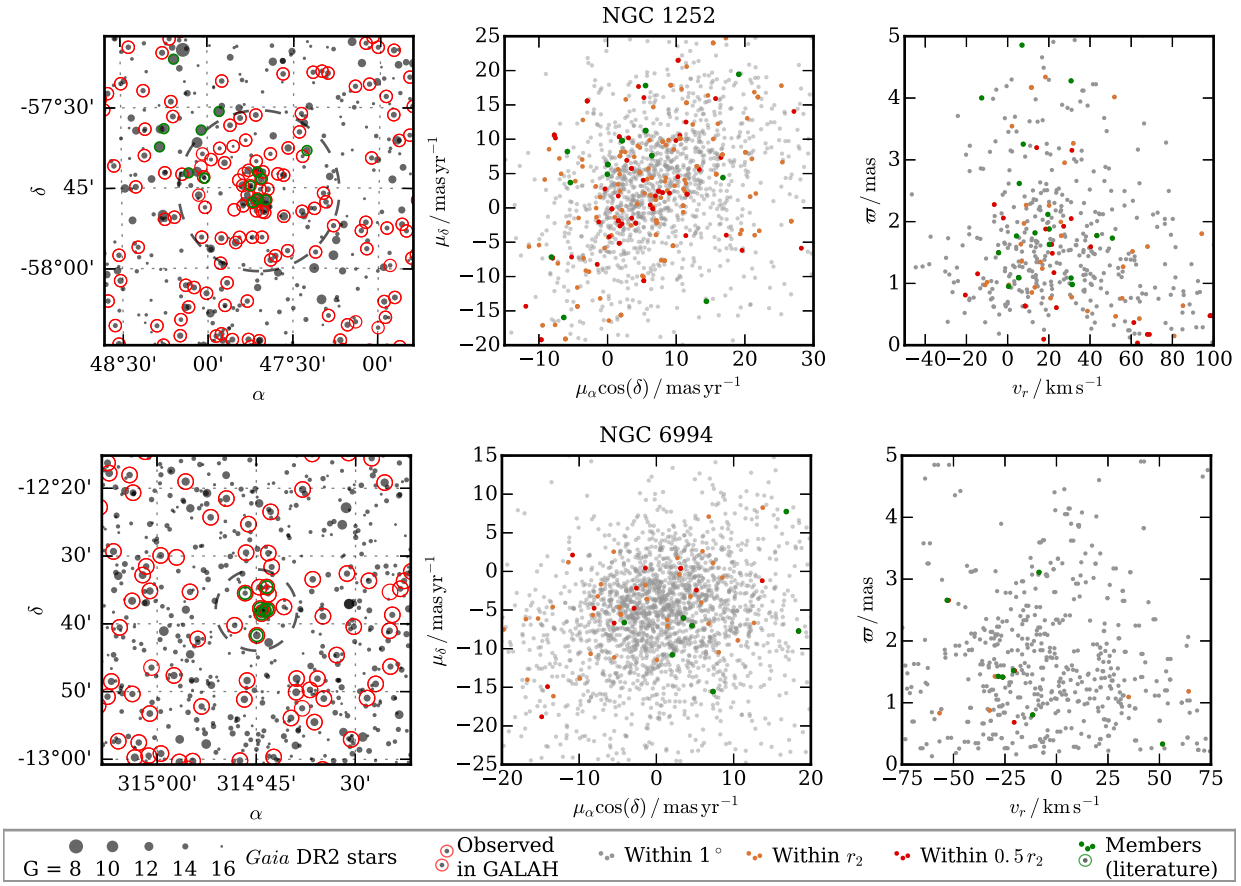

Figure 3. Six dimensional space for stars in and around NGC 1252 (top row) and NGC 6994 (bottom row). Left: Position of *Gaia* DR2 stars with magnitude G<16 (gray) with marked stars observed in the GALAH survey (circled in red) and faux members from the literature (circled in green). The dashed circle marks the cluster radius. Middle: *Gaia* DR2 proper motions for all stars inside a 1° radius from the cluster centre (gray), stars inside r_2 (orange), stars inside 0.5 r_2 (red), and faux members from the literature (green). Right: Radial velocity and proper motions for stars that have radial velocity measured either in *Gaia* DR2 or in the GALAH survey. Same colours are used as in the middle panel.

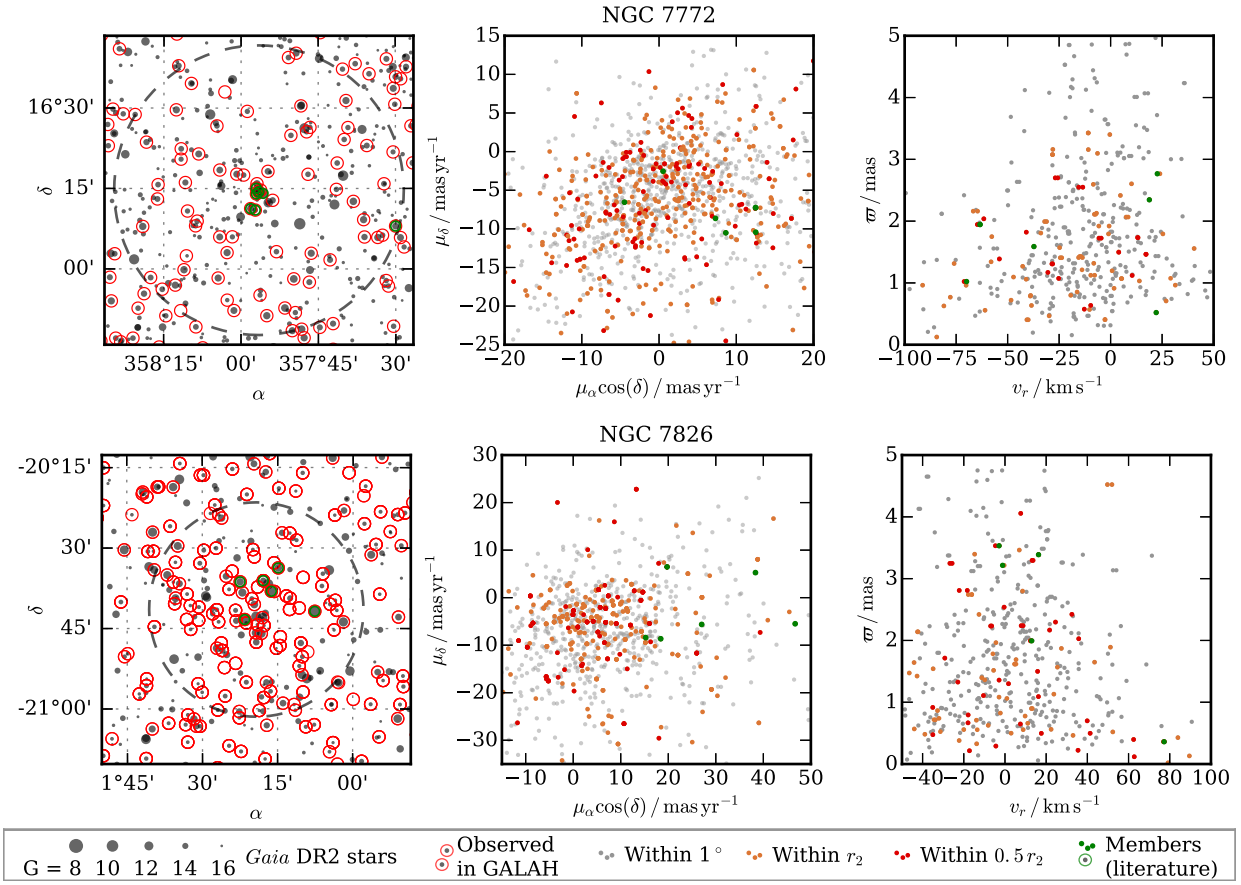

Figure 3. Continued for NGC 7772 (top row) and NGC 7826 (bottom row).

Table 2. Final parameters for NGC 1901. Measurement uncertainties are given after the ± sign in the bottom row.

α	δ	l	b	r_0	r_1	r_2	r_c	r_t	$\mu_\alpha \cos(\delta)$	μ_δ	v_r	ϖ	dist.	σ_{v_r}	$\left[\frac{\text{Fe}}{\text{H}}\right]$	$\left[\frac{\alpha}{\text{Fe}}\right]$	log t
°	°	°	°	′	′	′	′	′	mas y^{-1}	mas y^{-1}	km s^{-1}	mas	pc	km s^{-1}	dex	dex	log yr
79.490	−68.342	278.914	−33.644	2.2	11.0	50.0	2.4	> 20	1.632	12.671	1.30	2.349	426.0	3.00	−0.32	0.11	8.26
±0.106	±0.031	±0.039	±0.043	±0.5	±2.5	±12.0	±0.7		±0.030	±0.018	±0.28	±0.009	±2.0	±0.27	±0.05	±0.05	±0.14

difference between the two quantities. We also measured the abundance of other elements and they are close to or above solar values. A total metallicity is therefore comparable to the one measured from the isochrone fitting.

NGC 1901 has been referred to as an open cluster remnant in the literature (e.g. by Carraro et al. (2007)). While there is no clear consensus on the classification an open cluster remnant, if an open cluster is sparsely populated with more than two-thirds of its initial stellar members lost, then a cluster like NGC 1901 is classed as a cluster remnant (Bica et al. 2001). However, as NGC 1901 is a rapidly dissolving cluster, it will not survive another pass through the Galactic plane in around 18 Myr. We used *galpy*[3] (Bovy 2015) to calculate the orbit of individual stars in the cluster. Currently the velocity dispersion of the cluster is 2.8 km s^{-1}. By the time the cluster passes the Galactic plane, the members will be spread out in a diameter ~8 times larger than they are now. This is enough that the cluster would be undetectable with the approach used in this paper.

[3] http://github.com/jobovy/galpy

Eggen (1996) referred to the NGC 1901 "supercluster", comprising a co-moving group of unbound stars associated with the cluster. NGC 1901 supercluster has been proposed to be dynamically related to the Hyades supercluster (the unbound group of stars co-moving with the Hyades open cluster), due to the similar space motions of the two groups (Dehnen 1998), and they are jointly referred to as Star Stream I by Eggen (1996). While the detection of the extended members of the NGC 1901 supercluster is beyond the scope of this paper, it is certainly plausible that the dispersed members of NGC 1901 are detectable within the Galactic motion space and can be used to gain insights into the dispersion mechanisms of the cluster.

4 DISCUSSION

Clusters cannot be simply split into high- and low-latitude, or sparse and rich clusters. There are a range of factors that could be specific to each cluster, depending on its initial mass, origin and evolutionary history. Furthermore, with typical cluster dispersion processes the

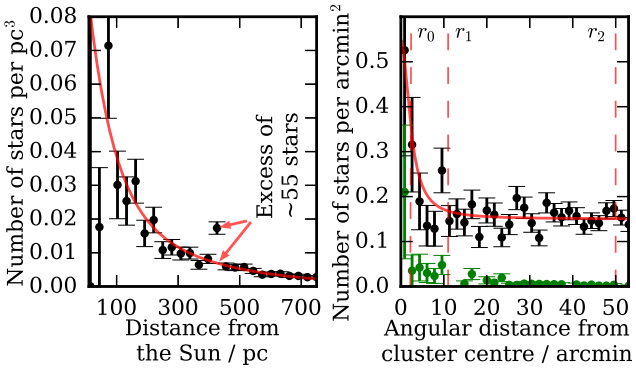

Figure 4. Left: Density of stars as a function of distance from the Sun. NGC 1901 produces a very significant signal at 426 pc. Stars in a 1° degree cone around the cluster centre are used for this plot. Right: Star density as a function of apparent distance from NGC 1901 centre. An overdensity above the background level (0.15 stars per arcmin^2) is clearly detected. Black points show measurements for all stars with magnitude G < 17 and green points only show the density of most probable members. Eyeballed radii r_0, r_1, and r_2 are marked. Red curve is a fitted King model.

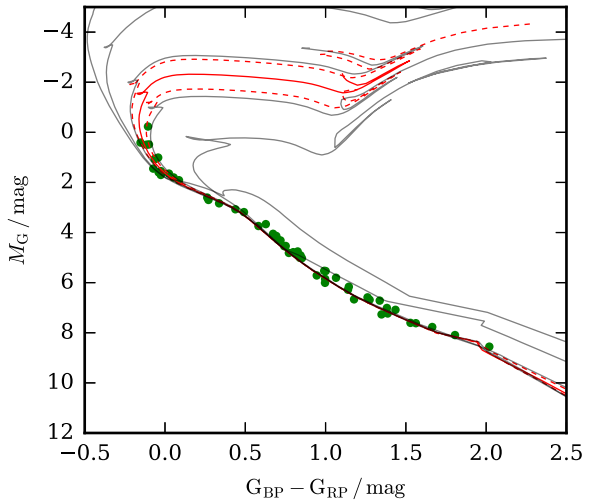

Figure 5. NGC 1901 members on the color-magnitude diagram. Magnitudes of the stars are corrected for extinction and color excess. If either is unavailable in *Gaia* DR2, we assumed a mean value for the cluster: $E(G_{BP} - G_{RP}) = 0.20$ and $A_G = 0.32$. Padova isochrones (Marigo et al. 2017) are plotted for log $t = 8.26$ (red solid curve), and for log $t = 8.12$ and log $t = 8.40$ (red dashed curves), all with [M/H] = −0.13. Isochrones for log $t = 7.0$, 7.5, 8.0, 8.5, and 9.0 are also plotted in gray. Varying the limiting membership probability within reasonable values does not add or remove any turn-off stars.

transition is smooth and there are other clusters similar to the ones described in this paper among the 39 clusters in our data set, such as Blanco 1 and NGC 1817. We chose not to include such clusters here because they are slightly more populated and closer to the plane than the clusters discussed above. Also, the cluster sample in our data set was not observed with a clear selection function, apart from trying to cover as wide range of ages and metallicities as possible. Hence one should not conclude that 4 out of 5 sparse high latitude clusters are not real. A lesson learned is that the existence of sparse clusters should be double-checked, regardless of how reputable are the respective cluster catalogues. Surveys of high-latitude clusters (Bica et al. 2001; Schmeja et al. 2014), after the *Gaia* parameters are included, will probably give a better picture.

It is expected that some sparse clusters are not real. The rate of faux clusters can be estimated from mean star densities and the number of possible members in the aggregation. Figure 6 shows the probability as a function of galactic latitude (a proxy for background star density) and the number of stars in the aggregation. We estimated the number of members from literature sources in each magnitude bin for the four faux clusters and we see that they all lie in the region where many faux clusters are expected to be found.

For NGC 1901 we found more members than one would find using the same literature as for the four faux clusters, so the position of NGC 1901 on plots in Figure 6 with respect to the faux clusters might not be completely representative. NGC 1901 also lies in front of the LMC, so the background count in the $G < 16$ panel is underestimated.

We can conclude that existence of the four false clusters has never been very plausible, since they were all discovered based on the star-counts only. Most probably, there are more long-known sparse clusters that will be disproved in the near future.

Gaia parameters are obviously proving to be well suited for cluster membership analysis, as well as for finding new clusters (Koposov et al. 2017; Castro-Ginard et al. 2018; Torrealba et al. 2018; Cantat-Gaudin et al. 2018; Dias et al. 2018). The fraction of reported clusters that are not real will probably be significantly less than in the past, but even in the *Gaia* era we can expect to find low-probability clusters that should be treated with caution. The same holds for membership probabilities. We show that positions, proper motions and distances are not enough and the whole 6D information must be used to find members with great certainty.

ACKNOWLEDGEMENTS

JK is supported by a Discovery Project grant from the Australian Research Council (DP150104667) awarded to J. Bland-Hawthorn and T. Bedding.

REFERENCES

Bassino L. P., Waldhausen S., Martínez R. E., 2000, A&A, 355, 138
Baumgardt H., Makino J., 2003, MNRAS, 340, 227
Bertelli Motta C., et al., 2018, preprint, (arXiv:1804.06293)
Bica E., Santiago B. X., Dutra C. M., Dottori H., de Oliveira M. R., Pavani D., 2001, A&A, 366, 827
Bouchet P., The P. S., 1983, Publications of the Astronomical Society of the Pacific, 95, 474
Bovy J., 2015, ApJS, 216, 29
Bovy J., 2016, ApJ, 817, 49
Buder S., et al., 2018, preprint, (arXiv:1804.06041)
Camargo D., Bica E., Bonatto C., 2016, A&A, 593, A95
Cantat-Gaudin T., et al., 2018, preprint, (arXiv:1805.08726)
Carraro G., 2000, A&A, 357, 145

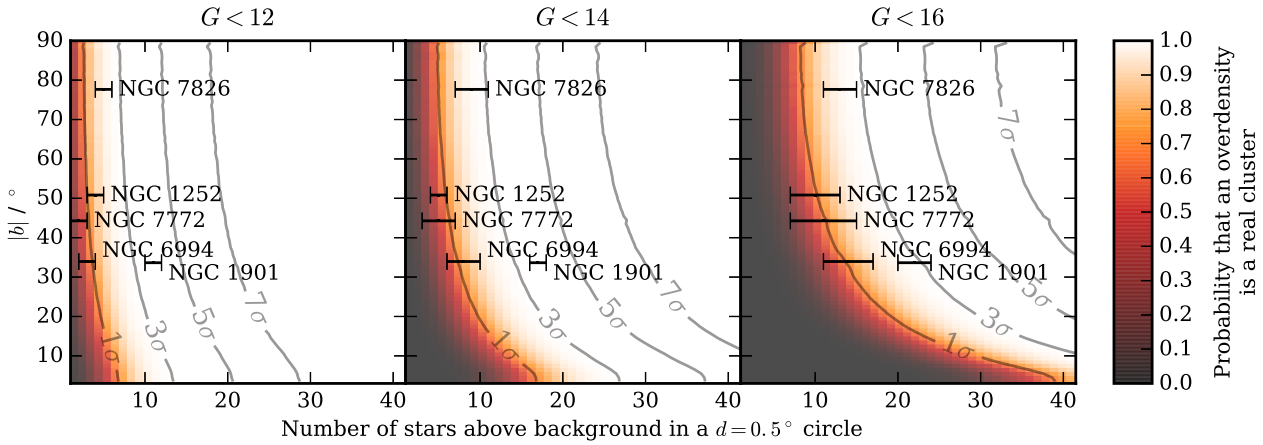

Figure 6. Probability that an overdensity of N stars above the background level in a 0.5° diameter circle is a real cluster. Panels show the probability for different magnitude cuts between $G < 12$ (left) and $G < 16$ (right). The probability changes significantly with the background level. Here we only show the variation as a function of absolute galactic latitude ($|b|$). Only minor differences in local density can be expected for regions around different clusters. Position of clusters studied in our work are indicated. For the nonexistent clusters we estimated the supposed number of stars from the literature sources. For all five clusters we assumed a radius of 0.25°, so all of them can be shown on the same plot.

Carraro G., 2002, A&A, 385, 471
Carraro G., de La Fuente Marcos R., Villanova S., Moni Bidin C., de La Fuente Marcos C., Baumgardt H., Solivella G., 2007, A&A, 466, 931
Castro-Ginard A., Jordi C., Luri X., Julbe F., Morvan M., Balaguer-Núñez L., Cantat-Gaudin T., 2018, preprint, (arXiv:1805.03045)
Chabrier G., 2003, PASP, 115, 763
Conrad C., et al., 2014, A&A, 562, A54
De Silva G. M., Sneden C., Paulson D. B., Asplund M., Bland-Hawthorn J., Bessell M. S., Freeman K. C., 2006, AJ, 131, 455
De Silva G. M., Freeman K. C., Asplund M., Bland-Hawthorn J., Bessell M. S., Collet R., 2007, AJ, 133, 1161
De Silva G. M., et al., 2015, MNRAS, 449, 2604
Dehnen W., 1998, AJ, 115, 2384
Dias W. S., Alessi B. S., Moitinho A., Lépine J. R. D., 2002, A&A, 389, 871
Dias W. S., Alessi B. S., Moitinho A., Lepine J. R. D., 2014, VizieR Online Data Catalog,
Dias W. S., Monteiro H., Assafin M., 2018, preprint, (arXiv:1805.11444)
Dreyer J. L. E., 1888, Memoirs of the Royal Astronomical Society, 49, 1
Eggen O. J., 1996, AJ, 111, 1615
Freeman K., Bland-Hawthorn J., 2002, ARA&A, 40, 487
Fujii M. S., Baba J., 2012, MNRAS, 427, L16
Gaia Collaboration Brown A. G. A., Vallenari A., Prusti T., de Bruijne J. H. J., Babusiaux C., Bailer-Jones C. A. L., 2018, preprint, (arXiv:1804.09365)
Gieles M., Bastian N., 2008, A&A, 482, 165
Gieles M., Athanassoula E., Portegies Zwart S. F., 2007, MNRAS, 376, 809
Gustafsson B., Church R. P., Davies M. B., Rickman H., 2016, A&A, 593, A85
Kereš D., Katz N., Weinberg D. H., Davé R., 2005, MNRAS, 363, 2
Kharchenko N. V., Piskunov A. E., Schilbach E., Röser S., Scholz R.-D., 2012, A&A, 543, A156
Kharchenko N. V., Piskunov A. E., Schilbach E., Röser S., Scholz R. D., 2013, A&A, 558
King I., 1962, AJ, 67, 471
Koposov S. E., Belokurov V., Torrealba G., 2017, MNRAS, 470, 2702
Kos J., et al., 2018, MNRAS, 473, 4612
Krumholz M. R., 2014, Phys. Rep., 539, 49
Marigo P., et al., 2017, ApJ, 835, 77
Martinez-Medina L. A., Pichardo B., Moreno E., Peimbert A., Velazquez H., 2016, ApJ, 817, L3
Martinez-Medina L. A., Pichardo B., Peimbert A., Moreno E., 2017, ApJ, 834, 58
Odenkirchen M., Soubiran C., 2002, A&A, 383, 163
Pavani D. B., Bica E., Dutra C. M., Dottori H., Santiago B. X., Carranza G., Díaz R. J., 2001, A&A, 374, 554
Sancisi R., Fraternali F., Oosterloo T., van der Hulst T., 2008, A&ARv, 15, 189
Schmeja S., Kharchenko N. V., Piskunov A. E., Röser S., Schilbach E., Froebrich D., Scholz R.-D., 2014, A&A, 568, A51
Sestito P., Randich S., Bragaglia A., 2007, A&A, 465, 185
Skrutskie M. F., et al., 2006, AJ, 131, 1163
Stryker L. L., 1993, PASP, 105, 1081
Torrealba G., Belokurov V., Koposov S. E., 2018, preprint, (arXiv:1805.06473)
de Silva G. M., Freeman K. C., Bland-Hawthorn J., Asplund M., Williams M., Holmberg J., 2011, MNRAS, 415, 563
de la Fuente Marcos R., de la Fuente Marcos C., Moni Bidin C., Carraro G., Costa E., 2013, MNRAS, 434, 194

Table A1. Coordinates, proper motions, parallax and radial velocity (where known) of NGC 1252 members from the literature. Not a single pair of stars can be found with matching parameters. Between all four sources the magnitude of stars extends from V=6.62 to V=17.97.

α °	δ °	$\mu_\alpha \cos(\delta)$ mas y^{-1}	μ_δ mas y^{-1}	ϖ mas	v_r km s^{-1}
		Members‡ in Kharchenko et al. (2013)			
47.4215	-57.6347	-0.03±0.05	4.90±0.04	0.95±0.03	0.5±0.6*
47.6764	-57.7014	-2.96±0.03	15.57±0.03	3.20±0.02	
47.2933	-57.7678	-1.07±0.06	-13.19±0.05	1.08±0.03	
48.0644	-57.6689	-4.70±0.05	3.90±0.05	1.39±0.03	
47.7155	-57.6683	1.57±0.05	-1.88±0.04	0.61±0.03	
47.9065	-57.5849	9.76±0.15	3.23±0.14	1.26±0.07	
48.0170	-57.7205	2.12±0.05	9.79±0.04	0.98±0.02	31.4±0.3†
47.3650	-57.6324	-3.59±0.10	12.80±0.09	1.72±0.05	
47.7089	-57.7856	0.04±0.05	6.32±0.04	1.63±0.03	20.3±0.8*
47.3982	-57.8135	6.42±0.04	4.39±0.03	0.76±0.02	
47.9903	-57.6525	4.39±0.14	9.04±0.14	1.49±0.07	
		Members in de la Fuente Marcos et al. (2013)			
47.6605	-57.7887	6.44±0.05	7.61±0.04	1.50±0.02	-4.4±1.1*
47.7356	-57.7966	5.55±0.04	11.25±0.03	1.09±0.02	5.3±0.2†
47.7498	-57.6912	9.95±0.08	9.81±0.07	0.85±0.05	
47.4953	-57.7548	3.06±0.10	10.20±0.09	0.66±0.05	
47.6336	-57.6454	3.49±0.05	5.74±0.05	0.81±0.03	
47.9003	-57.6730	13.01±0.03	6.05±0.03	2.26±0.02	
48.0170	-57.7205	2.12±0.05	9.79±0.04	0.98±0.02	31.4±0.3†
48.0104	-57.6817	5.09±0.07	-0.90±0.07	0.25±0.04	
		Members in Pavani et al. (2001)			
47.7089	-57.7856	0.04±0.05	6.32±0.04	1.63±0.03	20.3±0.8*
47.6868	-57.7234	-21.39±0.04	-44.09±0.04	1.88±0.02	20.1±1.5*
47.7680	-57.7731	-17.57±0.05	-18.16±0.05	2.05±0.03	
47.7356	-57.7966	5.55±0.04	11.25±0.03	1.09±0.02	5.3±0.2†
47.7498	-57.7446	31.21±0.03	17.01±0.03	1.77±0.02	43.3±4.4*
47.6764	-57.7014	-2.96±0.03	15.57±0.03	3.20±0.02	
47.7083	-57.7021	4.05±0.07	-69.89±0.06	11.87±0.04	54.0±0.3*
		Members in Bouchet & The (1983)			
47.7083	-57.7021	4.05±0.07	-69.89±0.06	11.87±0.04	54.0±0.3*
48.1091	-57.7038	35.61±0.04	1.30±0.04	1.73±0.02	50.8±0.2*
48.2607	-57.8339	1.19±0.07	-4.57±0.08	1.08±0.05	
48.2768	-57.6225	5.54±0.05	17.82±0.06	4.28±0.03	30.8±0.5*
48.2507	-57.5659	16.81±0.04	4.41±0.04	1.09±0.02	30.8±0.5*
48.0351	-57.5712	43.18±0.06	15.34±0.06	3.25±0.03	7.6±0.3*
47.9307	-57.5136	-5.85±0.04	8.20±0.04	2.12±0.02	19.5±0.2*
48.1921	-57.3504	-5.42±0.06	3.69±0.06	4.00±0.03	-12.6±0.5*
47.7845	-57.1932	-3.39±0.09	-26.14±0.10	4.86±0.05	7.0±0.5*
47.8202	-57.1590	19.11±0.24	19.46±0.23	1.77±0.13	4.3±0.3*
47.9257	-56.9778	-8.18±0.04	-7.17±0.04	1.82±0.02	13.3±0.2*
47.0998	-57.0100	14.40±0.04	-13.60±0.05	2.62±0.03	5.6±0.2*
48.7182	-57.8377	-6.38±0.08	-15.96±0.08	2.82±0.05	105.3±0.3*

‡ only members with probability>0.8
* v_r from *Gaia* DR2
† v_r from GALAH

APPENDIX A: LITERATURE MEMBERS FOR NGC 1252, NGC 6994, NGC 7772, AND NGC 7826

Tables A1 to A4 list members given in the literature for four disproved clusters. Only stars we were able to cross-match with *Gaia* DR2 are listed. These stars are of course not real members, but we use them to rest our case in Figure 3.

APPENDIX B: LIST OF PROBABLE NGC 1901 MEMBERS

In Table B1 we list most probable NGC 1901 members. Note that only stars in the *Gaia* DR2 are included. Figure B1 shows the position of most probable members on the sky.

This paper has been typeset from a TEX/LATEX file prepared by the author.

Table A2. Coordinates, proper motions, parallax and radial velocity (where known) of NGC 6994 members from the literature. Not a single pair of stars can be found with matching parameters. The magnitude of stars extends from V=10.35 to V=19.53.

α °	δ °	$\mu_\alpha \cos(\delta)$ mas y^{-1}	μ_δ mas y^{-1}	ϖ mas	v_r km s^{-1}
		Members in Bassino et al. (2000)			
314.7366	-12.6418	7.33±0.07	-15.55±0.05	1.41±0.04	-26.2±0.2*
314.7401	-12.6294	18.41±0.07	-7.72±0.06	2.66±0.05	-53.1±0.7*
314.7283	-12.6345	2.05±0.09	-10.80±0.07	3.11±0.06	-8.5±0.6*
314.7222	-12.6318	4.61±0.07	-7.03±0.05	1.52±0.04	-20.8±0.6*
314.8046	-12.6706	-21.38±0.05	-9.39±0.03	1.18±0.03	
314.7781	-12.5914	3.50±0.05	-6.02±0.03	0.80±0.03	-11.6±0.1†
314.7776	-12.5777	-11.40±0.07	1.19±0.05	1.91±0.05	
314.7423	-12.5768	-4.60±0.04	-5.57±0.03	0.83±0.03	
314.7237	-12.5765	-4.16±0.04	-6.62±0.03	0.33±0.03	51.5±0.1†
314.7378	-12.5785	-5.53±0.35	2.55±0.23	1.78±0.23	
314.7487	-12.6955	16.82±0.07	7.75±0.04	1.43±0.04	-28.2±1.6*

* v_r from *Gaia* DR2
† v_r from GALAH

Table A3. Coordinates, proper motions, parallax and radial velocity (where known) of NGC 7772 members from the literature. Not a single pair of stars can be found with matching parameters. Between both sources the magnitude of stars extends from V=11.08 to V=18.00.

α °	δ °	$\mu_\alpha \cos(\delta)$ mas y^{-1}	μ_δ mas y^{-1}	ϖ mas	v_r km s^{-1}
		Members‡ in Kharchenko et al. (2013)			
357.9917	16.2920	17.13±0.05	-8.65±0.02	1.39±0.03	
357.8054	16.1146	6.94±0.34	-2.56±0.14	1.30±0.16	
357.5001	16.1331	12.52±0.09	-10.44±0.04	2.77±0.04	22.7±1.7*
358.2582	16.4424	18.28±0.13	-14.25±0.06	1.03±0.07	
357.9434	16.2490	12.45±0.05	-7.38±0.02	1.88±0.03	
357.9288	16.2352	7.30±0.08	-8.65±0.04	0.52±0.04	22.1±0.3*
357.9052	15.9786	11.59±0.10	-7.66±0.04	1.05±0.05	
358.0828	16.2812	10.42±0.30	-6.91±0.18	1.53±0.15	
357.9428	16.2398	12.50±0.07	-7.25±0.04	1.95±0.04	-63.4±0.1†
358.3233	16.0572	16.19±0.09	-9.59±0.04	1.03±0.05	
		Members in Carraro (2002)			
357.9428	16.2398	12.50±0.07	-7.25±0.04	1.95±0.04	-63.4±0.1†
357.9690	16.1878	6.75±0.16	-38.26±0.08	5.48±0.09	-20.1±1.2*
357.9129	16.3036	-16.76±0.06	-31.33±0.03	2.04±0.03	
357.9506	16.2513	8.65±0.06	-10.52±0.03	1.02±0.03	-69.9±1.3*
357.9434	16.2490	12.45±0.05	-7.38±0.02	1.88±0.03	
357.8977	16.2136	-6.48±0.05	-18.50±0.02	0.64±0.03	
357.9503	16.2333	0.52±0.05	-2.54±0.03	2.34±0.03	18.8±0.2†
357.9917	16.2920	17.13±0.05	-8.65±0.02	1.39±0.03	
357.9367	16.2454	12.56±0.05	5.86±0.03	1.50±0.03	
357.9538	16.1833	-4.48±0.05	-6.55±0.03	1.59±0.03	-37.2±0.1†
357.9056	16.3006	2.74±0.08	0.49±0.04	0.48±0.04	

‡ only members with probability>0.8
* v_r from *Gaia* DR2
† v_r from GALAH

Table A4. Coordinates, proper motions, parallax and radial velocity (where known) of NGC 7826 members from the literature. Not a single pair of stars can be found with matching parameters. The magnitude of stars extends from V=9.72 to V=16.67.

α °	δ °	$\mu_\alpha \cos(\delta)$ mas y^{-1}	μ_δ mas y^{-1}	ϖ mas	v_r km s^{-1}
		Members‡ in Dias et al. (2002, 2014)			
1.3897	-20.8588	12.26±0.12	2.83±0.07	0.72±0.07	
1.1267	-20.6970	46.70±0.09	-5.49±0.06	3.22±0.06	-1.1±0.2*
1.2085	-20.6567	25.99±0.06	-11.67±0.04	1.30±0.03	
1.2711	-20.6347	15.25±0.07	-8.40±0.05	0.36±0.04	77.3±0.1†
1.2949	-20.7413	14.65±0.10	1.17±0.06	1.18±0.05	
1.2976	-20.6020	19.74±0.05	6.47±0.03	0.79±0.03	-17.8±0.1†
1.3595	-20.7226	38.34±0.12	5.27±0.06	3.39±0.05	16.3±0.7*
1.3745	-20.6056	27.03±0.07	-5.63±0.04	3.53±0.04	-2.9±0.1†
1.4658	-20.7048	16.05±0.05	-5.44±0.04	0.92±0.04	
1.2480	-20.5623	18.41±0.07	-8.65±0.05	1.99±0.04	12.9±1.1*
1.4210	-20.5883	12.84±0.08	1.43±0.04	2.54±0.04	

‡ only members with probability>0.9
* v_r from *Gaia* DR2
† v_r from GALAH

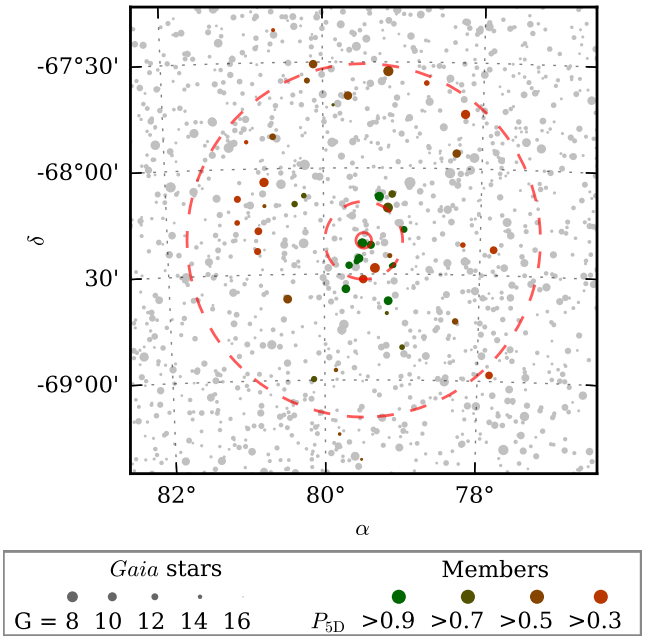

Figure B1. Positions of most probable NGC 1901 members. All *Gaia* DR2 stars with $G < 16$ are plotted in grey and the members are plotted in colour. Radii r_0, r_1, and r_2 are marked with red circles.

Table B1. List of most probable NGC 1901 members ordered by probability. Probability P_{5D} is given to all stars in *Gaia* DR2 with known position, proper motions and parallax. The uncertainty of all measurements is properly taken into the account. Stars with known radial velocity are given another probability (P_{6D}) based on their radial velocity as well. Stars for which the radial velocity is measured by GALAH are marked with an asterisk.

Gaia DR2 source id	α	δ	r	$\mu_\alpha \cos(\delta)$	μ_δ	ϖ	G	v_r	P_{5D}	P_{6D}
	°	°	°	mas y^{-1}	mas y^{-1}	mas	mag	km s^{-1}		
4658338537313572096	79.5799	-68.4403	0.1037	1.490	12.736	2.368	12.48	1.43*	0.980	0.979
4658335518014051712	79.6781	-68.4590	0.1360	1.666	12.592	2.324	11.49	3.01*	0.972	0.938
4658765564465430272	79.3346	-68.1278	0.2218	1.727	12.684	2.333	14.78		0.964	
4658338747829382528	79.5499	-68.4267	0.0875	1.425	12.620	2.340	10.33	-0.49*	0.963	0.926
4658340053499327360	79.3992	-68.3630	0.0395	1.792	12.825	2.388	10.81	-11.58*	0.960	0.124
4658714677689040640	79.5087	-68.3554	0.0150	1.709	12.942	2.331	9.21		0.943	
4658384751164454016	79.1349	-68.4621	0.1775	1.558	12.617	2.360	13.52		0.943	
4658384755525236864	79.1097	-68.4584	0.1821	1.703	12.647	2.357	12.72	6.07	0.931	0.704
4658333422070733312	79.7205	-68.5703	0.2435	1.652	12.869	2.323	10.37	-4.09*	0.927	0.647
4658726218241467008	79.6766	-68.0353	0.3144	1.819	12.558	2.361	10.40		0.912	
4658765736264109312	79.2926	-68.1346	0.2199	1.700	12.537	2.282	9.74	0.95*	0.910	0.909
4658378570770738944	79.2189	-68.5038	0.1900	1.404	12.759	2.367	16.14		0.899	
4658329298899347328	79.1740	-68.6263	0.3070	1.655	12.778	2.290	10.21		0.891	
4658388260218178048	78.9761	-68.2895	0.1970	1.671	12.729	2.398	11.98	54.53*	0.887	0.000
4658766114221175040	79.1298	-68.1230	0.2565	1.888	12.597	2.367	11.34	1.61*	0.878	0.877
4658328680424119552	79.1905	-68.6844	0.3596	1.834	12.825	2.391	14.23		0.874	
4658751030294843776	79.5615	-67.9204	0.4225	1.749	12.950	2.382	15.04		0.786	
4658709970404987904	79.9753	-68.4676	0.2184	1.453	12.870	2.434	15.89		0.762	
4658349364997640064	78.9891	-68.8448	0.5350	1.885	12.586	2.309	13.02		0.757	
4658764499313514112	79.1826	-68.1872	0.1921	1.911	12.461	2.443	9.03		0.737	
4658760822820870144	79.8711	-67.7024	0.6553	1.586	12.884	2.409	14.73		0.727	
4658748109717269120	80.1748	-67.9189	0.4940	1.447	12.760	2.395	16.20		0.723	
4658733335028239232	80.2483	-68.1295	0.3524	1.458	12.684	2.430	13.04		0.716	
4658383033177728512	78.8183	-68.3973	0.2537	1.783	12.413	2.330	16.77		0.696	
4658732265555421952	80.3665	-68.1686	0.3681	1.416	12.418	2.375	12.39	13.68*	0.678	0.102
4658286069991771392	80.1431	-68.9948	0.6947	1.648	12.546	2.349	12.56	-1.51	0.678	0.615
4658764877270576000	79.0623	-68.1334	0.2620	1.703	13.032	2.426	8.79		0.672	
4658332631796592768	79.7948	-68.5810	0.2639	1.478	12.252	2.385	9.83		0.659	
4658761887972710144	79.6859	-67.6594	0.6865	1.438	12.987	2.285	10.41	1.87*	0.650	0.648
4658385305280833152	79.1563	-68.4135	0.1422	1.372	13.111	2.354	13.53		0.620	
4658765736264108800	79.2927	-68.1340	0.2205	1.372	12.756	2.234	12.85		0.617	
4658758963072125312	79.8855	-67.7579	0.6025	1.624	13.071	2.357	12.34	4.11*	0.598	0.542
4658693507772922624	80.4737	-68.6163	0.4533	1.496	12.385	2.307	10.21	-1.14	0.596	0.554
4658854002110866688	80.1928	-67.5869	0.7998	1.436	12.488	2.348	12.79	3.71	0.591	0.550
4658854831036783232	80.1141	-67.5098	0.8646	1.472	12.744	2.327	10.52	-11.26*	0.590	0.084
4658286933330473600	79.8546	-68.9528	0.6250	1.621	12.260	2.324	14.00		0.588	
4658198766214889856	79.0002	-69.1475	0.8248	1.663	12.347	2.382	15.76		0.578	
4658293083726796928	79.2046	-69.0403	0.7059	1.731	12.339	2.344	16.96		0.574	
4658191172772162944	79.5185	-69.3746	1.0326	1.596	12.702	2.394	14.90		0.572	
4658779342721084160	78.9703	-67.8583	0.5211	1.641	12.620	2.266	17.35		0.562	
4658806005880090368	78.9761	-67.6454	0.7227	1.817	12.884	2.433	15.14		0.553	
4658336548806471936	79.4965	-68.5243	0.1823	1.578	12.169	2.310	10.41	-0.96*	0.551	0.518
4658812053194570240	79.1862	-67.5435	0.8066	1.636	12.858	2.237	8.80		0.528	
4658709553769767424	80.3100	-68.1705	0.3488	1.666	12.974	2.329	17.56		0.528	
4658275659025982592	79.8104	-69.2550	0.9203	1.367	12.346	2.364	14.52		0.515	
4658377810497066368	78.8767	-68.5252	0.2905	1.717	12.960	2.257	17.61		0.500	
4658337820116699648	79.3460	-68.4719	0.1403	1.348	12.174	2.299	9.13		0.491	
4658743608590786432	80.6294	-67.8497	0.6504	1.407	12.880	2.412	12.16	1.82*	0.483	0.481
4658785493114963328	78.3230	-67.9287	0.5997	1.871	12.932	2.328	10.51	1.53	0.478	0.477
4658730070853284608	80.7501	-68.1758	0.4955	1.269	12.647	2.367	14.24		0.443	
4658360458826656128	78.3023	-68.7202	0.5762	1.624	13.046	2.347	12.35	7.36	0.430	0.273
4658737423838030080	80.7492	-68.0642	0.5439	1.417	12.714	2.252	9.66		0.422	
4658727528232702976	80.8333	-68.2937	0.4986	1.316	12.636	2.272	11.23	0.98*	0.418	0.417
4658188350951010560	78.9303	-69.3897	1.0669	1.831	12.295	2.309	15.28		0.406	
4658515700465243392	80.8487	-68.3891	0.5031	1.281	12.411	2.306	11.87	1.63*	0.384	0.383
4658380799796398464	78.8235	-68.4930	0.2879	1.810	12.475	2.360	18.33		0.380	
4658276728485892224	80.0309	-69.2272	0.9066	1.584	12.259	2.277	16.15		0.379	
4658162241856515712	78.7408	-69.5461	1.2338	1.636	12.438	2.368	15.65		0.367	
4658540989235266176	81.1009	-68.2522	0.6024	1.425	12.754	2.358	13.07		0.353	
4658833321873098368	80.9618	-67.8727	0.7221	1.375	12.874	2.411	14.04		0.345	
4658548337881959424	81.0902	-68.1410	0.6263	1.523	12.747	2.430	11.91	0.82*	0.325	0.325
4658797244146158976	78.2421	-67.6328	0.8495	1.813	12.513	2.330	17.56		0.325	
4658316173421984128	80.3508	-68.7060	0.4814	1.281	12.454	2.310	18.02		0.319	
4658515631745778944	80.8804	-68.3981	0.5156	1.180	12.752	2.380	16.06		0.312	
4658794838964513792	78.2221	-67.7434	0.7636	2.022	12.619	2.279	9.74	-3.73*	0.308	0.225